

# Modification of the hole injection barrier in organic light-emitting devices studied by ultraviolet photoelectron spectroscopy

X. M. Ding

Center of Super-Diamond and Advanced Films (COSDAF) and Department of Physics and Materials Science, City University of Hong Kong, Hong Kong, China and Surface Physics Laboratory (National Key Laboratory), Fudan University, Shanghai 200433, China

L. M. Hung, L. F. Cheng, Z. B. Deng, X. Y. Hou, C. S. Lee,<sup>a)</sup> and S. T. Lee

Center of Super-Diamond and Advanced Films (COSDAF) and Department of Physics and Materials Science, City University of Hong Kong, Hong Kong, China

(Received 22 December 1999; accepted for publication 13 March 2000)

Ultraviolet photoelectron spectroscopy has been applied to the investigation of modified hole injection barriers in organic light-emitting devices (OLEDs). Different from those reported previously, the indium tin oxide (ITO) surface treated *in situ* by oxygen plasma possesses a work function of 5.2 eV, and the organic ITO interface thereafter formed shows a 0.5 eV smaller hole injection barrier compared to that on untreated ITO. Insertion of an ultrathin SiO<sub>2</sub> layer between the organic and ITO results in a similar reduction of the barrier. This indicates that improved hole injection favors efficient operation of OLEDs, as manifested by enhanced efficiency by the SiO<sub>2</sub> insertion. © 2000 American Institute of Physics. [S0003-6951(00)02219-1]

The organic light-emitting device (OLED) is currently considered a promising candidate for low-cost, full-color flat-panel displays. Continuous effort has been made to enhance brightness and efficiency of the device ever since Tang and Van Slyke reported the first vacuum-deposited, molecule-based OLED in 1987.<sup>1</sup> Aiming at optimizing charge injection and transport, quite a number of studies were focused on improving the cathode/electron transport layer (ETL) structure,<sup>2-7</sup> as it was thought that the current conduction and quantum efficiency were mainly controlled by electron trapping in the ETL for the most extensively investigated molecule-based OLEDs.<sup>8</sup> More recently, the anode/hole transport layer (HTL) structure has attracted considerable attention, as well.<sup>9-11</sup> By adopting an ultrathin SiO<sub>2</sub> layer sandwiched between the anode and the HTL, Deng *et al.* have succeeded in fabricating the OLED with much enhanced performance.<sup>10</sup> The formation of an improved electronic structure at the HTL/anode interface is likely the reason for the performance enhancement in such a device, but the exact role of the SiO<sub>2</sub> layer is unclear.

In this letter, we report a photoemission study of the SiO<sub>2</sub>-sandwiched HTL/anode structure. The valence-band photoelectron spectra measured show that the presence of the SiO<sub>2</sub> layer can result in a 0.5–0.7 eV reduction of the hole injection barrier. This, combined with the results measured from the HTL/anode interfaces with the anode surface treated by oxygen plasma (OP) exposure or some other methods, confirms that the SiO<sub>2</sub>-induced performance enhancement can be ascribed to the more efficient hole injection across the lowered barrier.

Experiments were carried out in a multifunctional ultra-high vacuum (UHV) system consisting of several analysis chambers and a sample preparation chamber. The analysis chamber used in the present study was equipped with the

facilities for ultraviolet photoelectron spectroscopy (UPS) and Auger electron spectroscopy (AES). In the preparation chamber, there were OP and organic evaporation sources for *in situ* sample treatment and HTL deposition, respectively. Same as in Ref. 10, the anode and hole transport materials were indium tin oxide (ITO) and *N,N'*-bis-(1-naphyl)-*N,N'*-diphenyl-1,1'-biphenyl-4,4'-diamine (NPB), respectively, and the SiO<sub>2</sub> deposition was conducted in a separate chamber by means of electron beam evaporation.

After routine chemical cleaning, the ITO-covered glass substrates were further treated by either OP or ozone exposure. Then, some of the samples were just kept in the chamber for immediate NPB deposition or annealing, and some were transferred to the separate chamber for SiO<sub>2</sub> deposition. The samples having experienced the different treatments were all covered with a 2 nm thick NPB layer finally. UPS spectra were taken both before and after the NPB deposition, so the effects of various predeposition treatments on the interfacial electronic structure were detected. The deposition rates of SiO<sub>2</sub> and NPB were monitored by quartz oscillators; and for SiO<sub>2</sub>, the exact thickness was further checked by AES. For UPS measurements, HeI( $h\nu = 21.22$  eV) was used as the excitation source and the samples were  $-4$  V biased.

*In situ* AES measurements showed that, following the OP treatment, carbon contaminants on the ITO surface were reduced to a small fraction of that on the as-loaded sample. Subsequent moderate annealing at temperatures lower than 350 °C in UHV resulted in the appearance of a sharp-featured valence band structure with a clearly observable Fermi edge in the UPS spectrum, as shown in Fig. 1. Such a well-defined valence band spectrum was not available from ITO surfaces prepared by other methods. So the binding energies of all the UPS spectra in this letter were referenced to the Fermi level determined from the spectrum of the ITO surface treated by OP exposure and annealing (OPA). By measuring the width of the spectrum, work function (WF) of

<sup>a)</sup>Electronic mail: apcslee@cityu.edu.hk

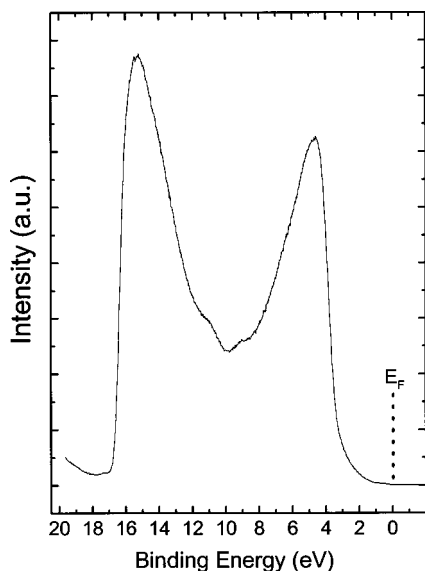


FIG. 1. UPS spectrum taken from the *in situ* OPA-treated ITO surface.

the surface was derived to be 4.4 eV. This value was much the same as those measured from most of the other ITO surfaces, but 0.8 eV lower than that measured immediately after the OP treatment. Table I summarizes the WFs measured from all of these surfaces.

Figure 2 shows the UPS spectra taken after the NPB deposition on the respective surfaces as listed in Table I. The well-separated multippeak structure is characteristic of molecular orbitals of the organic material.<sup>12</sup> Similar to determination of WFs of the ITO substrates, one can derive from the width of the spectra in Fig. 2 that ionization potential (IP) of NPB is 5.2 eV, exactly the same as reported previously.<sup>13</sup> By examining the positions of the molecular orbital peaks and the threshold of the highest occupied molecular orbital (HOMO), the barrier height, expressed as the separation between the HOMO threshold and the Fermi level  $E_F$  of ITO, can be determined for the differently treated NPB/ITO interfaces. It is obvious that the higher the substrate work function, the lower the barrier height. The lowest barrier height here is 0.7 eV, emerging from immediate deposition of NPB onto the *in situ* OP-treated ITO surface with a WF of 5.2 eV. All the barrier height values are also listed in Table I for comparison.

It is interesting to notice that although there exists a close relation between the barrier height and the ITO work function as shown in Table I, the barrier height is not exactly equal to the difference between the IP of NPB and the WF of ITO. In other words, the vacuum levels of the two sides of

TABLE I. WF of ITO following different pretreatments and barrier height appearing at the NPB/ITO interface subsequently formed. The latter is measured as the energetic separation between  $E_F$  of ITO and HOMO threshold of NPB.

Treatment	WF(eV)	$E_F$ -HOMO(eV)
As-loaded or vacuum annealing	4.4	1.2
<i>Ex situ</i> ozone exposure	4.6	1.0
Ozone exposure+annealing	4.5	1.1
<i>In situ</i> oxygen plasma exposure	5.2	0.7
Oxygen plasma exposure+annealing	4.4	1.2

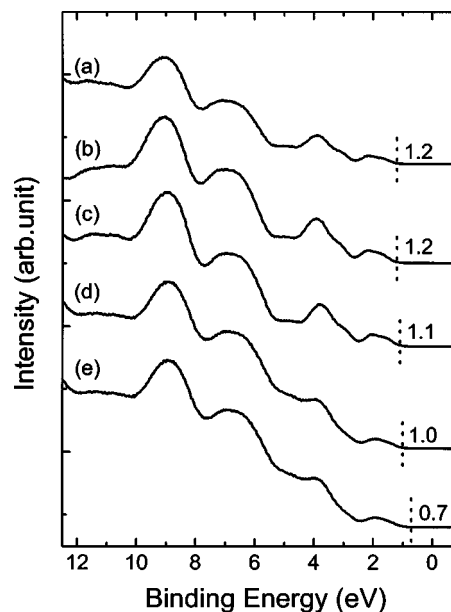


FIG. 2. UPS spectra of NPB/ITO with the ITO substrates (a) air exposed or vacuum annealed, (b) *in situ* OPA treated, (c) ozone exposed and annealed, (d) *ex situ* ozone exposed, and (e) *in situ* OP exposed.

the NPB/ITO interface are not aligned at the same height. The existence of interfacial dipoles in such an organic/ITO system can thus be expected.

Figure 3 shows the UPS spectra measured from the NPB/ITO interfaces where the ITO substrates were precov-  
ered with a SiO<sub>2</sub> layer of 0.3, 1.0, and 2.5 nm, respectively, and then briefly exposed to the air before the NPB deposition. Different from the cases of NPB deposited on bare air-exposed ITO surfaces, now the barrier heights are 0.7, 0.6, and 0.5 eV, respectively. That means the sandwiched SiO<sub>2</sub> layer has the same effect as the *in situ* OP treatment in modifying the interfacial electronic structure and can result in a reduction in the barrier height for more than 0.5 eV.

It has long been recognized that the OP or ozone treat-

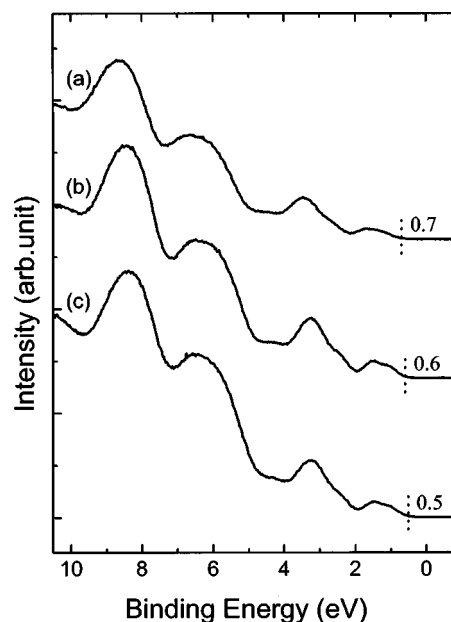


FIG. 3. UPS spectra of NPB/ITO with the presence of a sandwiched SiO<sub>2</sub> layer (a) 0.3, (b) 1.0, and (c) 2.5 nm thick.

ment of the ITO substrate is practically important to the fabrication of OLEDs and that the operating voltage of OLEDs can be reduced by plasma treatment of the ITO anode.<sup>14</sup> But the exact effect of such treatments on the formation of the hole injection barrier has not been fully clear. Actually, there exist conflicting reports in the literature on whether the WF of the ITO surface would change upon the OP treatment: While Park *et al.*<sup>15</sup> and Nuesch *et al.*<sup>16</sup> did not find such a change in their photoemission measurements, Wu *et al.*,<sup>14</sup> Osada *et al.*,<sup>17</sup> and Mason *et al.*<sup>18</sup> confirmed the existence of the treatment-induced barrier height changes. It seems to us that whether the relation between the treatments and the barrier height can be observed or not depends to a large extent on the experimental conditions. The main difference between the previous and present photoemission experiments is that, in the present case, the measurements have been performed *in situ*. It is thus likely that brief exposure to the air after the OP treatment was the reason for smearing the WF variation in the previous experiments. We have actually observed such a phenomenon in our present experiment. The fact that the barrier height will no longer be the same if the OP-treated sample is briefly air exposed before the NPB deposition reflects the instability of the surface dipole formed upon the OP treatment. Temporal accumulation of negatively-charged oxygen ions on the ITO surface, which hinders escape of electrons from the surface and hence increases the work function, may readily be destroyed either by annealing or by air exposure. In this sense, insertion of an ultrathin solid buffer<sup>10</sup> or further treating the surface with acids<sup>11</sup> favors the formation of a stable dipole layer which may ease the injection of the holes from the anode. One may notice that, in Fig. 3, the barrier height decreases monotonically with increasing SiO<sub>2</sub> thickness in the thickness range investigated. This explains why the electroluminescent (EL) efficiency of the device optimizes at the SiO<sub>2</sub> thickness of about 1 nm.<sup>10</sup> The sandwiched SiO<sub>2</sub> layer may have a dual thickness dependence on the EL efficiency: On one hand, increase of the layer thickness in the nanometer range may enhance the hole injection efficiency due to the decrease of the barrier height; on the other hand, however, increased layer thickness leads to an increased series resistance, which in turn hampers EL efficiency enhancement.

In summary, we have shown by UPS that both oxygen plasma exposure and SiO<sub>2</sub> insertion can lead to a significant reduction of the hole injection barrier in the OLEDs with ITO as the anode. While the barrier height induced by oxygen plasma may be readily smeared upon air exposure, the effect of the SiO<sub>2</sub> layer is quite stable. This explains why significant enhancement in brightness and efficiency can be achieved when a SiO<sub>2</sub>-sandwiched anode structure is used in molecule-based OLEDs.

This work was supported by a Strategic Research Grant of the City University of Hong Kong (Project No. 7000967).

- <sup>1</sup>C. W. Tang and S. A. VanSlyke, *Appl. Phys. Lett.* **51**, 913 (1987).
- <sup>2</sup>L. S. Hung, C. W. Tang, and M. G. Mason, *Appl. Phys. Lett.* **70**, 152 (1997).
- <sup>3</sup>F. Li, H. Tang, J. Andereg, and J. Shinar, *Appl. Phys. Lett.* **70**, 1233 (1997).
- <sup>4</sup>G. E. Jabbour, Y. Kawabe, S. E. Shaheen, J. F. Wang, M. M. Morrell, B. Kippelen, and N. Peyghambarian, *Appl. Phys. Lett.* **71**, 1762 (1997).
- <sup>5</sup>G. E. Jabbour, B. Kippelen, N. R. Armstrong, and N. Peyghambarian, *Appl. Phys. Lett.* **73**, 1185 (1998).
- <sup>6</sup>J. Kido and Y. Lizumi, *Appl. Phys. Lett.* **73**, 2721 (1998).
- <sup>7</sup>J. Kido and T. Matsumoto, *Appl. Phys. Lett.* **73**, 2866 (1998).
- <sup>8</sup>P. E. Burrows, Z. Shen, V. Bulovic, D. M. McCarty, S. R. Forrest, J. A. Cronon, and M. E. Thompson, *J. Appl. Phys.* **79**, 7991 (1996).
- <sup>9</sup>C. Giebeler, H. Antoniadis, D. D. C. Bradley, and Y. Shirota, *J. Appl. Phys.* **85**, 608 (1999).
- <sup>10</sup>Z. B. Deng, X. M. Ding, S. T. Lee, and W. A. Gambling, *Appl. Phys. Lett.* **74**, 2227 (1999).
- <sup>11</sup>Q. T. Le, F. Nuesch, L. J. Rothberg, E. W. Forsythe, and Y. Gao, *Appl. Phys. Lett.* **75**, 1357 (1999).
- <sup>12</sup>K. Sugiyama, D. Yoshimura, T. Miyamae, T. Miyazaki, H. Ishii, Y. Ouchi, and K. Seki, *J. Appl. Phys.* **83**, 4928 (1998).
- <sup>13</sup>S. T. Lee, Y. M. Wang, X. Y. Hou, and C. W. Tang, *Appl. Phys. Lett.* **74**, 670 (1999).
- <sup>14</sup>C. C. Wu, C. I. Wu, J. C. Sturm, A. Kahn, *Appl. Phys. Lett.* **70**, 1348 (1997).
- <sup>15</sup>Y. Park, V. Choong, Y. Gao, B. R. Hsieh, and C. W. Tang, *Appl. Phys. Lett.* **68**, 2699 (1996).
- <sup>16</sup>F. Nuesch, L. J. Rothberg, E. W. Forsythe, Q. T. Le, and Y. Gao, *Appl. Phys. Lett.* **74**, 880 (1999).
- <sup>17</sup>T. Osada, Th. Kugler, P. Broms, W. R. Salaneck, *Synth. Met.* **96**, 77 (1998).
- <sup>18</sup>M. G. Mason, L. S. Hung, C. W. Tang, S. T. Lee, K. W. Wong, and M. Wang, *J. Appl. Phys.* **86**, 1688 (1999).